U.S. Department of Transportation

Federal Railroad Administration

Wheel Bearing Brake/Instrumented Wheelset Friction Characterization Study

Office of Research,
Development
and Technology
Washington, DC 20590

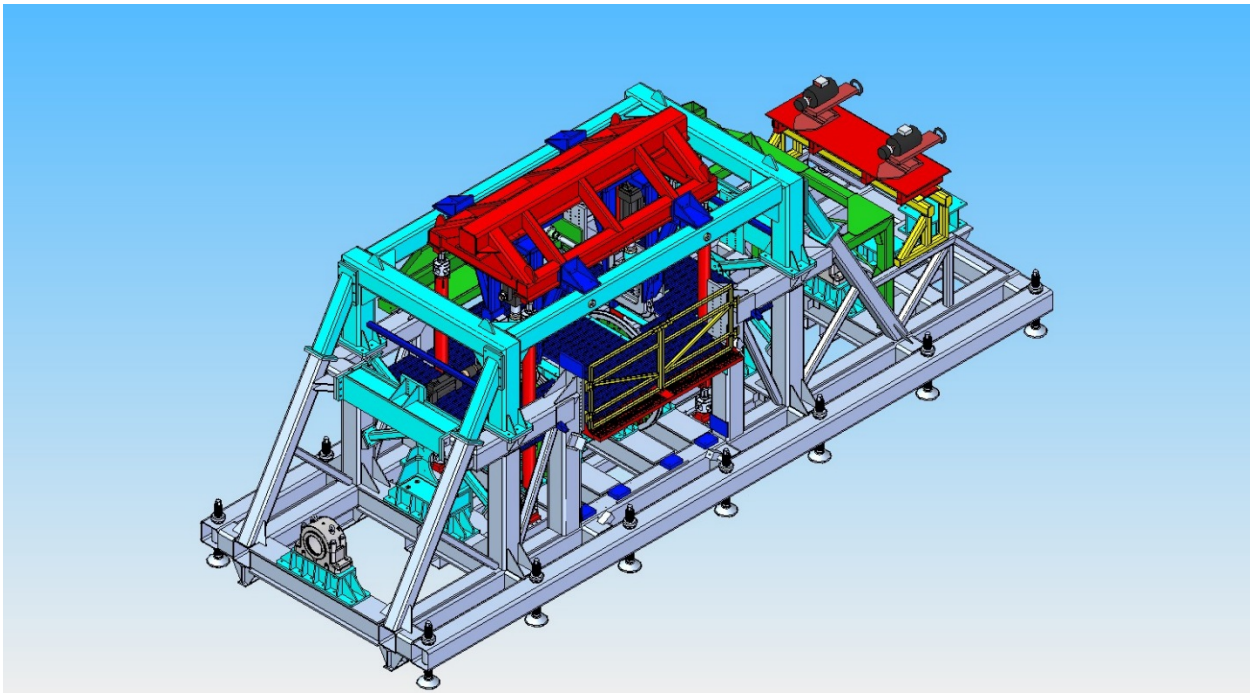

DOT/FRA/ORD-19/46

Final Report
December 2019

NOTICE

This document is disseminated under the sponsorship of the Department of Transportation in the interest of information exchange. The United States Government assumes no liability for its contents or use thereof. Any opinions, findings and conclusions, or recommendations expressed in this material do not necessarily reflect the views or policies of the United States Government, nor does mention of trade names, commercial products, or organizations imply endorsement by the United States Government. The United States Government assumes no liability for the content or use of the material contained in this document.

NOTICE

The United States Government does not endorse products or manufacturers. Trade or manufacturers' names appear herein solely because they are considered essential to the objective of this report.

REPORT DOCUMENTATION PAGE

Form Approved
OMB No. 0704-0188

Public reporting burden for this collection of information is estimated to average 1 hour per response, including the time for reviewing instructions, searching existing data sources, gathering and maintaining the data needed, and completing and reviewing the collection of information. Send comments regarding this burden estimate or any other aspect of this collection of information, including suggestions for reducing this burden, to Washington Headquarters Services, Directorate for Information Operations and Reports, 1215 Jefferson Davis Highway, Suite 1204, Arlington, VA 22202-4302, and to the Office of Management and Budget, Paperwork Reduction Project (0704-0188), Washington, DC 20503.

1. AGENCY USE ONLY (Leave blank)	2. REPORT DATE	3. REPORT TYPE AND DATES COVERED
	December 2019	Technical Report 6/1/2013 to 12/31/2016

4. TITLE AND SUBTITLE
Wheel Bearing Brake/Instrumented Wheelset (WBB/IWS) Friction Characterization Study

5. FUNDING NUMBERS
FR-RPD-0054-13-01-00

6. AUTHOR(S)
Daniel Szablewski, Robert Caldwell

7. PERFORMING ORGANIZATION NAME(S) AND ADDRESS(ES)
National Research Council Canada
2320 Lester Road, Building U-89
Ottawa, ON, Canada K1V 1S2

8. PERFORMING ORGANIZATION REPORT NUMBER

9. SPONSORING/MONITORING AGENCY NAME(S) AND ADDRESS(ES)
U.S. Department of Transportation
Federal Railroad Administration
Office of Railroad Policy and Development
Office of Research, Development and Technology
Washington, DC 20590

10. SPONSORING/MONITORING AGENCY REPORT NUMBER
DOT/FRA/ORD-19/46

11. SUPPLEMENTARY NOTES
COR: Ali Tajaddini

12a. DISTRIBUTION/AVAILABILITY STATEMENT
This document is available to the public through the FRA website.

12b. DISTRIBUTION CODE

13. ABSTRACT (Maximum 200 words)

The wheel/rail (W/R) interface experiences variable friction conditions during in-service operation. This is due mainly to the application of top-of-rail friction modifiers, gage face lubricants, and other third-body materials that exist at the W/R interface due to non-controlled environmental factors (e.g., rain, ice, plants, etc.). Friction acts to modify the traction coefficient (Tc) (i.e., creep curve) at the W/R contact zone. Understanding creep curve behavior as a function of friction is critical to providing accurate numerical modelling boundary condition inputs of wheel response during train operation. Accurate numerical modelling of train operations allows optimization of in-service component life cycles, maximizing safe operations of these components and minimizing detrimental environmental impacts. The study was aimed at mapping out Tc behavior as a function of four friction conditions: dry, wet, lube stick, and top of rail friction modification stick, applied directly on the wheel tread surface. In addition, vertical loading and wheel speed were investigated. Creep curve saturation results were presented independently as a function of each input condition. Wear and rolling contact fatigue were assessed as well on the wheel running surface following each friction condition run.

14. SUBJECT TERMS
Wheel/rail interface, W/R, friction, angle of attack, AoA, traction curves, instrumented wheelset, IWS, rolling contact fatigue, wear, tribometer

15. NUMBER OF PAGES
38

16. PRICE CODE

17. SECURITY CLASSIFICATION OF REPORT	18. SECURITY CLASSIFICATION OF THIS PAGE	19. SECURITY CLASSIFICATION OF ABSTRACT	20. LIMITATION OF ABSTRACT
Unclassified	Unclassified	Unclassified	

NSN 7540-01-280-5500 Standard Form 298 (Rev. 2-89)

METRIC/ENGLISH CONVERSION FACTORS

ENGLISH TO METRIC	METRIC TO ENGLISH
LENGTH (APPROXIMATE)	**LENGTH** (APPROXIMATE)
1 inch (in) = 2.5 centimeters (cm)	1 millimeter (mm) = 0.04 inch (in)
1 foot (ft) = 30 centimeters (cm)	1 centimeter (cm) = 0.4 inch (in)
1 yard (yd) = 0.9 meter (m)	1 meter (m) = 3.3 feet (ft)
1 mile (mi) = 1.6 kilometers (km)	1 meter (m) = 1.1 yards (yd)
	1 kilometer (km) = 0.6 mile (mi)
AREA (APPROXIMATE)	**AREA** (APPROXIMATE)
1 square inch (sq in, in^2) = 6.5 square centimeters (cm^2)	1 square centimeter (cm^2) = 0.16 square inch (sq in, in^2)
1 square foot (sq ft, ft^2) = 0.09 square meter (m^2)	1 square meter (m^2) = 1.2 square yards (sq yd, yd^2)
1 square yard (sq yd, yd^2) = 0.8 square meter (m^2)	1 square kilometer (km^2) = 0.4 square mile (sq mi, mi^2)
1 square mile (sq mi, mi^2) = 2.6 square kilometers (km^2)	10,000 square meters (m^2) = 1 hectare (ha) = 2.5 acres
1 acre = 0.4 hectare (he) = 4,000 square meters (m^2)	
MASS - WEIGHT (APPROXIMATE)	**MASS - WEIGHT** (APPROXIMATE)
1 ounce (oz) = 28 grams (gm)	1 gram (gm) = 0.036 ounce (oz)
1 pound (lb) = 0.45 kilogram (kg)	1 kilogram (kg) = 2.2 pounds (lb)
1 short ton = 2,000 pounds (lb) = 0.9 tonne (t)	1 tonne (t) = 1,000 kilograms (kg) = 1.1 short tons
VOLUME (APPROXIMATE)	**VOLUME** (APPROXIMATE)
1 teaspoon (tsp) = 5 milliliters (ml)	1 milliliter (ml) = 0.03 fluid ounce (fl oz)
1 tablespoon (tbsp) = 15 milliliters (ml)	1 liter (l) = 2.1 pints (pt)
1 fluid ounce (fl oz) = 30 milliliters (ml)	1 liter (l) = 1.06 quarts (qt)
1 cup (c) = 0.24 liter (l)	1 liter (l) = 0.26 gallon (gal)
1 pint (pt) = 0.47 liter (l)	
1 quart (qt) = 0.96 liter (l)	
1 gallon (gal) = 3.8 liters (l)	
1 cubic foot (cu ft, ft^3) = 0.03 cubic meter (m^3)	1 cubic meter (m^3) = 36 cubic feet (cu ft, ft^3)
1 cubic yard (cu yd, yd^3) = 0.76 cubic meter (m^3)	1 cubic meter (m^3) = 1.3 cubic yards (cu yd, yd^3)
TEMPERATURE (EXACT)	**TEMPERATURE** (EXACT)
[(x-32)(5/9)] °F = y °C	[(9/5) y + 32] °C = x °F

QUICK INCH - CENTIMETER LENGTH CONVERSION

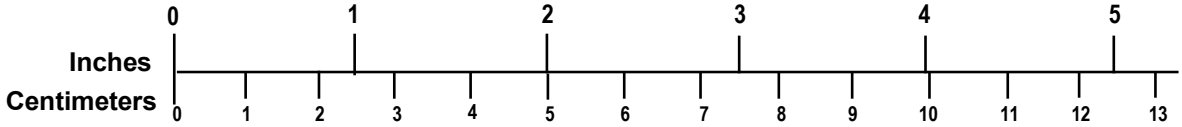

QUICK FAHRENHEIT - CELSIUS TEMPERATURE CONVERSIO

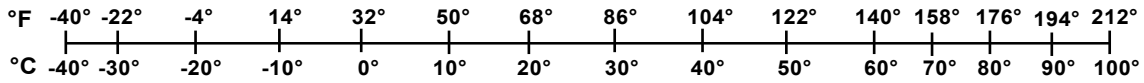

For more exact and or other conversion factors, see NIST Miscellaneous Publication 286, Units of Weights and Measures. Price $2.50 SD Catalog No. C13 10286

Updated 6/17/98

Acknowledgements

The authors want to thank the Federal Railroad Administration for support in this research endeavor and the TTX Company for facilitating the use of their Instrumented Wheel Set (IWS) for this work. In addition, the authors thank Eric Magel, Principal Engineer at National Research Council Canada, for providing initial ideas on conducting this research project.

Contents

Illustrations

Tables

Executive Summary

The wheel/rail (W/R) interface experiences variable friction conditions during in-service operation. This is due mainly to the application of top-of-rail friction modifiers (TOR FM) and gage face (GF) lubricants, and other third-body materials that exist at the W/R interface due to non-controlled environmental factors (e.g., rain, ice, foliage or plants, etc.). Friction acts to modify the traction coefficient (Tc) at the W/R contact zone. Understanding Tc behavior as a function of friction is critical to providing accurate numerical modelling boundary condition inputs of wheel response during train operation. Accurate numerical modelling of train operations allows optimization of in-service component life cycles, maximizing safe operations of these components and minimizing detrimental environmental impacts.

The Federal Railroad Administration funded experiments that the National Research Council (NRC) Canada carried out on a full-size wheelset operating on rotating rollers to simulate the in-service behavior of W/R interaction. The testing occurred on the NRC's wheel bearing and brake (WBB) test facility at the Automotive and Surface Transportation (AST) Ottawa, Ontario campus.

During experimentation researchers varied independently the friction, wheelset vertical loading, roller speed, and wheelset angle of attack (AoA) to study the effects of these conditions on creep curve behavior and in particular to identify creep curve saturation points for each set of conditions. The objective was to provide modelling experts with real-world creep curve data, in particular the peak Tc, to feed the numerical models and make them more accurate for predicting in-service wheel operation. This would increase the reliability and confidence of predictions made through these models.

Testing showed that applying AoA to the wheelset wears off the lube and TOR FM stick materials relatively quickly, whereas the wet condition saturated very early on and stabilized quickly compared to stick material application. In addition, lube and TOR FM stick application saturated at a much higher AoA than wet condition and did not stabilize at any specific AoA. The material wear-off rate was faster than the replenishing rate. This was particularly a problem at lowest test speed of 2 mph. The stick material deposition, which was saturated ahead of the 2 mph test runs wore off quickly with application of AoA and could not be replenished on the interface at rate equal to or greater than its rate of use. As such, at 2 mph roller speed stick material application resulted in relatively similar peak Tc as in "dry" friction conditions. Future creep tests at lower roller speeds should take into account the amount of the product deposition per W/R contact unit area to match the deposition rates achieved at higher speeds. This would ensure similar stick material product availability at the W/R interface across multiple testing conditions, and make low and high roller speed tests more comparable.

The wet runs carried out at 2 mph, on the other hand, had an issue with effectively saturating the W/R interface at such low roller speed. Water was not effectively saturating the W/R interface thereby causing the interface to remain mostly dry. This is evidenced by the peak Tc "wet" condition values, which were very similar to the "dry" condition values at the same roller speed.

At higher roller speeds dry test runs had the higher peak Tc values, whereas wet runs had the lowest peak Tc, with stick material application peak Tc values in between these extremes (see Table 1 in the report).

Peak Tc was not very sensitive to vertical load changes, and the values remained relatively unchanged in the 10 to 37.5 kip range for the specific friction and roller speed combinations investigated. This was also the case for roller speed, where the peak Tc was relatively constant in the 10 to 37.5 kip vertical load range.

Roller speed had no effect on the lateral loads in any of the friction and vertical load conditions. Response was on average flat in the 2-30 mph roller speed range for all frictions and vertical loads applied during the test. However, lateral load differences were observed between the +ve and –ve AoA sweeps. These effects could have been due to either spin creep (i.e., differences in spin creep between the AoA sweep in the direction of roller travel versus AoA sweep in the direction opposite of roller travel) or roller and/or wheelset small diameter differences between opposing wheels, either of which would contribute to a force acting with or opposite to the direction of AoA sweep, thereby resulting in increasing or decreasing lateral forces.

Since only one wheelset and one set of rollers was used thorough the entire experiment the contributing amount of such small diameter differences could not be determined with all certainly. Future work could focus on employing multiple wheelsets and/or rollers with varying diameters to help quantify the effect of diameter changes on lateral loads.

Despite these challenges the benefits of the full-size testing carried out at WBB cannot be overemphasized. The testing carried out provided full-scale creepage datasets for simulation work of train operation. This in turn will allow prediction of realistic tractive effort at the W/R interface in variable train operating environments. As such, the testing carried out in this study contributes to the body of knowledge in the area of W/R interaction by providing a database of realistic wheelset operating environments and resulting peak tractive effort.

1. Introduction

Investigating the influence of friction modification on full-size wheel/rail system is relatively expensive and not easily attainable. This is due mostly to industry's lack of access to necessary instrumentation capable of evaluating the wheel/rail (W/R) relationship on a full size wheelset in a controlled environment. To date one study carried out on a full size rig addressed rolling contact fatigue (RCF) development [1]. However, most testing is done on scaled down test rigs, which are either pin-on-disk [3] or twin-disk [4] test machines. Both of these are scaled down laboratory versions of the W/R contact mechanism.

National Research Council (NRC) Canada has the capabilities to test full-size wheelsets in heavy axle load (HAL) environment, and took upon itself the task of evaluating variable friction conditions under different wheel loading, roller speed, and angle-of-attack (AoA). All this in an effort to develop traction curves (Tc) (i.e., the relationship between wheel traction and AoA as a function of friction, load, and rolling speed).

Results presented in this report summarize the experimental setup, testing methodology, and outcomes from variable test runs. Culmination of this testing is development of a table summarizing peak Tc values, one for each set of variable input conditions.

1.1 Background

Friction has been demonstrated to have a controlling influence on nearly all aspects of wheel/rail (W/R) interaction, including wear [1, 3, 4], fatigue [1, 4], corrugation [2, 4], noise [2, 4], and derailments due to low rail rollover and wheel climb. It is also influenced by railhead debris and water trapped at the interface, leading to development of surface oxidation [5–7].

Traditionally, gage face (GF) lubrication has been utilized to decrease the friction level between the wheel flange and the high rail gage corner to minimize wear in both components, and to reduce the propensity for a wheel to climb up the gage face of the rail. Recently, top-of-rail friction modifiers (TOR FM) have been applied on TOR running surfaces to reduce lateral forces and minimize wear and rolling contact fatigue (RCF) damage on both high and low TOR surfaces in curves. These materials are being applied in both liquid form through wayside application or in solid stick form by onboard train application.

Although tangible rail and wheel life-extension benefits of both GF lubrication and TOR FM technologies have been demonstrated in railroad operations over time, these technologies are in many cases not optimized for in-service operating conditions. Some in-field studies show that real friction coefficient is not constant and is surprisingly low (0.10–0.25) when water-based TOR FM is used, and is dependent on amount of modified applied at the interface [8]. As overuse of modifiers can impact train braking distance, it is beneficial to optimize their use to target specific performance attributes. As such, there is substantial room for improvement in understanding when and how much of the modifier should be applied at the interface. Developing an understanding of Tc for variable modifiers as a function of applied AoA is a step in that direction.

Numerical modelling of train operations is utilized as a way of predicting wheel and rail component service life by simulating wear and RCF damage. These models rely heavily on assumptions about train operations, wheel and rail response to friction levels among them. To date these numerical models oversimplify friction by applying simplified approaches and

assumptions. By providing actual experimental evidence of W/R behavior at different friction levels the authors aim to make these models more accurate, such that they better represent actual W/R contact conditions in the field.

To allow better representation of W/R contact conditions for numerical models the National Research Council Canada (NRC) conducted studies of full-size W/R interaction at variable loads, speeds, angles-of-attack (AoA), and friction conditions. This investigation addressed the effect of friction conditions on creep forces generated at the W/R interface. The overall goal of this study was to provide real-world boundary condition saturation creep values to feed numerical simulation models of friction at the W/R interface, thereby to increase the reliability and confidence of predictions made through these numerical models.

The results of the study have the potential to make numerical modelling more effective, minimize unsafe and costly W/R operating environments, and improve the economic and environmental benefits of wheel and rail maintenance and investments as well as to optimize power unit fuel consumption and minimize energy loss in railway vehicles.

1.2 Objectives

The objective of this study was to develop real-world creep values under four distinct friction conditions (dry, wet, lubricated, and friction-managed) for variable wheel loads, speeds and AoA values.

1.3 Overall Approach

The research approach consists of full-scale laboratory testing, followed by analysis of the data.

The laboratory testing was accomplished using an instrumented freight railroad wheelset on a rolling test rig. Commercially available dry-stick friction products were continuously applied to the wheels to produce the lubricated and friction-managed test conditions. A stream of water was directed into the W/R interface at both wheels to produce the wet test condition. An instrumented wheelset (IWS) measured creep forces in the W/R interface. A hand-operated tribometer measured the coefficient of friction on the surface of one roller at the lowest test speed. Transverse profile measurements of the wheels and rollers were recorded before initial testing and after testing was complete for each friction condition, to track wear.

Following the tests, the measured data was post-processed and analyzed to develop traction versus creepage curves and values of peak lateral and longitudinal forces and traction coefficients, for each test condition.

1.4 Scope

The major tasks of the research include:

- Laboratory measurements of W/R friction parameters under 35 different conditions
- Data analysis and reporting

The outcomes of this project are peak (or saturation) traction coefficient values (tabular and plotted), plots of traction creep curves versus AoA for the tested conditions, plots of peak lateral and longitudinal force for the tested conditions, and plots of roller coefficient of friction values the tested conditions at the lowest test speed only.

1.5 Organization of the Report

This report has a thorough review of the test activities, results and conclusions. The report is organized as follows:

1. Introduction
2. Problem Description
3. Results
4. Conclusion

2. Problem Description

The IWS measures the lateral and longitudinal creep forces and the normal load at the W/R interface of each wheel at variable wheelset loads, roller speeds, applied AoA, and interface friction conditions. The relationships between these individual inputs are then defined to generate full traction versus creepage curves for all test conditions simulated. In addition, the roller and wheel wear and RCF conditions are assessed following the application of each friction state. Also, a correlation is developed between the tribometer coefficient-of-friction (COF) readings versus the applied AoA at 2 mph roller speed at the four investigated friction conditions.

Three vertical loads (10, 15, and 37.5 kilopounds [kip]) and 3 roller speeds (2, 10, and 30 mph) were applied at each of the 4 friction conditions for a total of 35 distinct test runs (see Figure 1). The dry friction condition of 37.5-kip vertical load, 30 mph speed run was not performed as it was deemed to excessively damage the wheel running surface at high angles of attack. A typical IWS setup in the WBB test rig is shown in Figure 2.

Each of the 35 test runs was executed several times to establish a consistency of IWS output response between individual runs. The data presented in this report represents the best run of the 2–3 runs executed at each test condition. As such, the experimental results presented here are a relatively accurate representation of the wheelset response at the W/R interface for the tested conditions.

- **Dry**
- **Lube Stick**
- **TOR Stick**
- **Wet**

X

Static Vertical Actuator Load [lb]	Roller Speed [mph]		
	2	**10**	**30**
37,500	**x**	**x**	**x**
15,000	**x**	**x**	**x**
10,000	**x**	**x**	**x**

= 35 Runs Total

Figure 1. Typical test run for a given test

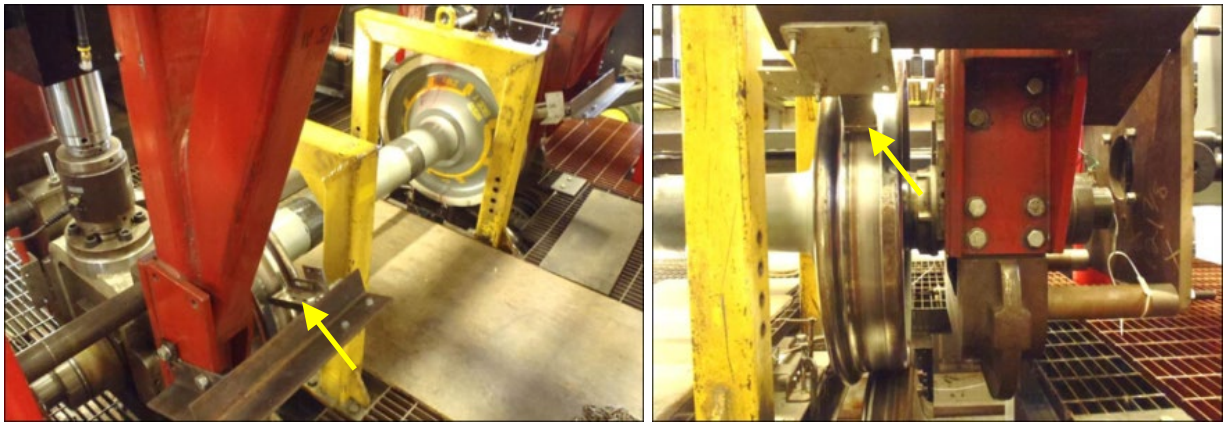

Figure 2. IWS setup in the WBB test rig

During the investigation IWS and WBB vertical, lateral, and longitudinal reaction loads and positions were acquired. This information was then utilized to process the data using IMC FAMOS© software, where the acquired data was filtered and smoothed. Creep curves were then

generated and peak values for all runs were compared to yield trends in the results based on friction, vertical loading, and roller speed inputs.

Testing results were analyzed using the IMC FAMOS© software package. Each set of data was initially processed using a power spectral density (PSD) function to determine the cutoff frequency best-suited for data filtering. These cutoff frequencies were then applied to each run to process the data. Further data smoothing was conducted to help select peak saturation traction coefficient (Tc) values in each graph.

The resulting plots included peak values for lateral forces as a function of friction, applied vertical load and roller speed, longitudinal forces as a function of friction, and Tc as a function of friction, load and speed.

During the course of testing the wheel and roller profiles were acquired using a MiniProf® following each friction run (e.g., post-dry, post-lube stick, post-TOR FM stick, post-wet). These profiles were then overlaid on the original wheel and roller profiles to track the amount of wear during testing. Results from this analysis are presented in the report. In addition, RCF on the wheel and roller running surfaces was assessed following each friction run. Findings from this analysis are also presented in the report.

Roller friction was measured for each friction condition at 2 mph roller speeds while the ±16 milliradian (mrad) AoA sweeps were applied to generate friction versus AoA plots. These are included in Section 3 of this report. The project was carried out using an IWS and a portable rolling contact tribometer to assess friction behaviors under several controlled conditions designed to simulate the revenue service environments.

The WBB consists of a pair of 63-inch rotating rollers that mimic moving rails and are capable of speeds up to 30 mph. A 28-inch diameter freight railway wheelset was mounted in a load frame that was situated in an overhead, flexibly mounted reaction table above the rotating rollers. Hydraulic actuators attached to the wheelset applied vertical and transverse loads, whereas AoA control was achieved through an electric motor attached to the wheel bearings via longitudinal arms. This setup allowed for precise control of wheel load conditions at the W/R interface during experimentation.

During testing, equipment settings were verified by sensors on the WBB that measured vertical, lateral, and longitudinal loads, and lateral wheel displacement. In addition, the WBB applied an AoA to the wheels by forcing the wheelset to yaw relative to the rollers about the center of the axle.

IWS outputs were utilized during experimental runs to measure reaction forces and positions at the W/R interface. This data was utilized during the analysis stage.

Both lube and TOR FM conditions were applied on the wheel tread running surface through dry stick application. The stick holder was positioned perpendicular to the wheel tread surface (see yellow arrows in Figure 2). Product was applied continuously during the AoA sweeps.

The yaw angle sweep of 0 → +16 → 0 → -16 → 0 mrad was performed at each test condition. Initially, the test was run without dwelling at the 0 mrad position. However, initial results indicated that following the positive AoA sweep, the dry stick material had worn off from the running surface to the point where the wheel was essentially “dry” when returned back to the 0 AoA position. Thereby, friction saturation condition was not available for subsequent negative AoA sweep. The ‘dry’ friction condition was verified with tribometer measurements, and it

prompted a modification of the test plan to include dwelling at 0 mrad for 5,000 revolutions of the wheelset in the lube and TOR FM stick application conditions, which allowed re-saturation of the friction condition for the negative AoA run. In each case, the saturation level at the wheel was verified through tribometer measurements at the roller using a 2 mph roller speed. Figure 3 illustrates a typical yaw AoA sweep applied in all lube and TOR FM dry stick test runs. The transition zone of 0 mrad was held for 5,000 revolutions of the wheelset, as indicated in the figure. Wet and dry runs were performed without the dwell at 0 mrad since the W/R interface was always "saturated" at these friction conditions (i.e., was always either dry or wet, depending on which condition was tested at the time).

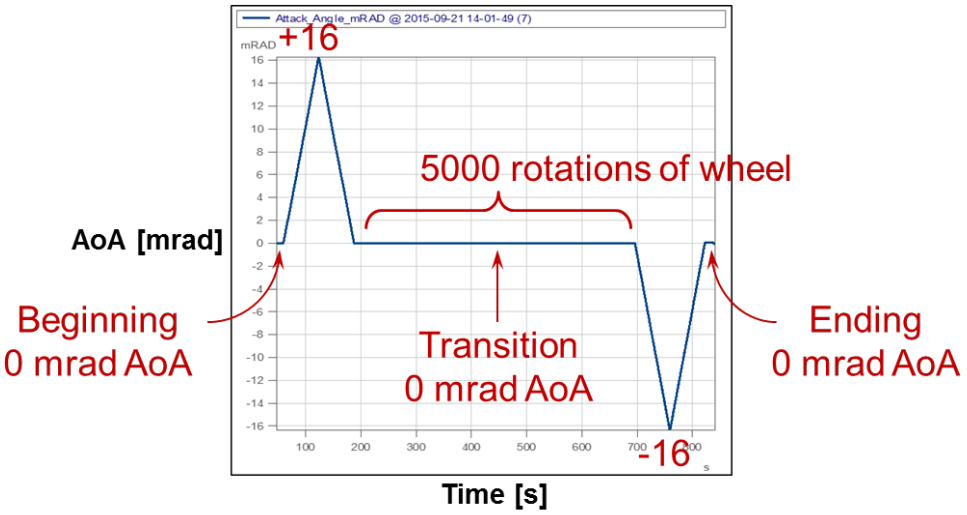

Figure 3. Schematic of a typical AoA sweep

All tribometer readings on the roller surface were taken at 2 mph roller speed in the 3 load conditions and the 4 friction conditions (total of 12 runs). A continuous +16 to -16 mrad yaw angle sweep was used during each tribometer run. In addition, wheel and roller profiles were acquired using the MiniProf®. The running surface condition of both the rollers and the wheelset was inspected following each friction condition run using dye penetrant.

2.1 Data Acquisition, Filtering, and Plotting

IWS channel data was acquired at 200 Hz and then filtered using IMC FAMOS® software for lateral and longitudinal force comparison and creep curve generation. PSD graphs were used to determine the cut-off frequency when filtering data for IWS vertical, lateral, and longitudinal forces. A Butterworth low-pass signal processing filter was used to filter the following IWS load response output datasets:

- F_{Lat}: Lateral Force
- F_{Vert}: Vertical Force
- F_{Long}: Longitudinal Force

The resulting data from these individual channels was then used in calculating Tc creep curves. Additional smoothing was applied to the creep curves to allow a more accurate selection of peak saturation values in negative and positive AoA sweeps.

Data filtering parameters were established by conducting an analysis of frequency cutoff points for each set of data. This was accomplished through PSD graph analysis (see Figure 4). During this procedure, the cutoff frequency of 0.3 Hz was selected for the lateral and longitudinal force output channels, and a cutoff frequency of 0.5 Hz was selected for the vertical force output channel. This allowed relatively accurate filtering of datasets while minimizing shifting of the data due to the filtering procedure.

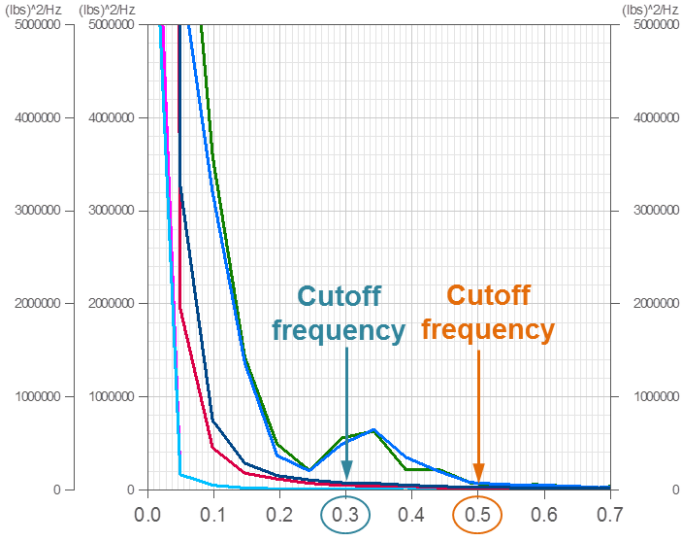

Figure 4. PSD graph of lateral, longitudinal, and vertical forces acquired from IWS force output channels. 0.3 and 0.5 Hz cutoff frequency limits utilized in Butterworth low-pass filtering procedure are indicated.

Examples of IWS unfiltered (200 Hz) vertical force outputs are presented on the left in Figure 5 in the wet friction condition for 10, 15, and 37.5 kip vertical forces at 2, 10, and 30 mph roller speeds. The filtered datasets are presented on the right of Figure 5 using the cutoff frequency limits shown in Figure 4. The filtering process generated more useful graphs, where peak values of each set of conditions could be readily identified. This data filtering was applied to all test runs in this experiment.

Wet condition, vertical load of **10 kip** at roller speeds of **2**, **10**, and **30** mph

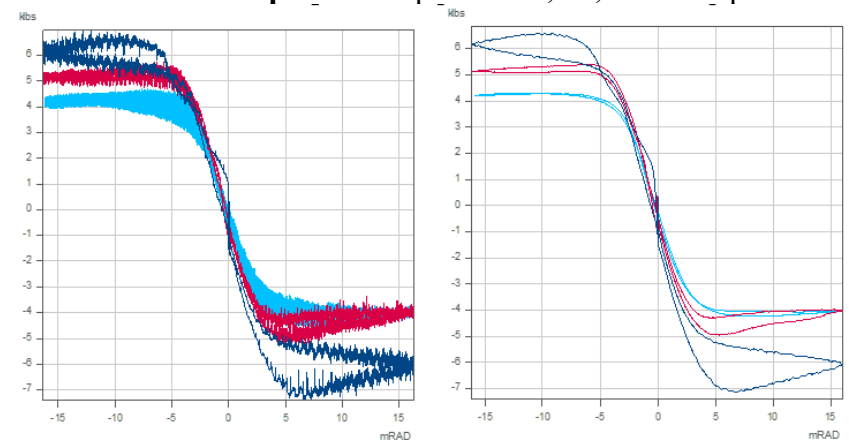

Wet condition, vertical load of **15 kip** at roller speeds of **2**, **10**, and **30** mph

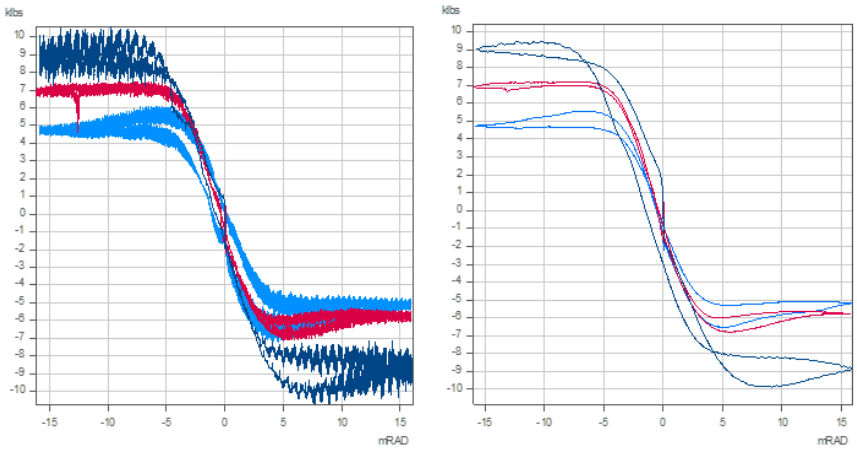

Wet condition, vertical load of **37.5 kip** at roller speeds of **2**, **10**, and **30** mph

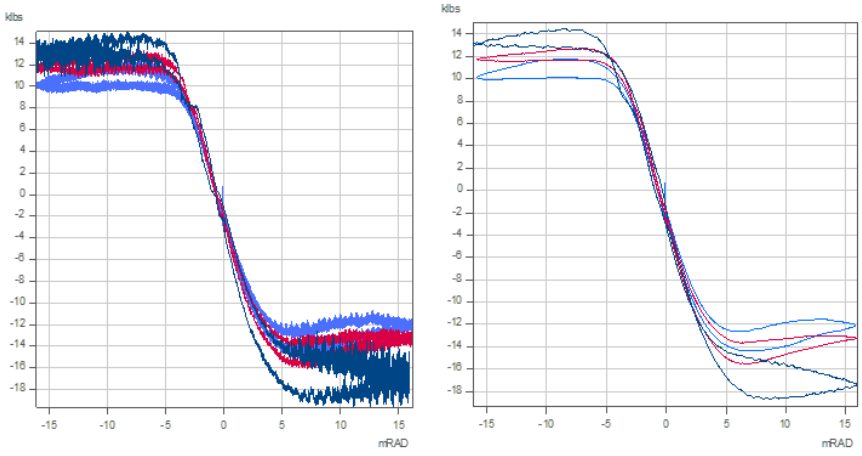

Figure 5. IWS vertical load data filtering indicating unfiltered (left) versus filtered (right) datasets for wet run conditions

2.2 Traction Coefficient Calculations

Data was processed in this way for F_{Long}, F_{Lat}, and F_{Vert} IWS channel outputs. Traction coefficient was then calculated using the following equation:

$$\mathrm{Tc} = \frac{\sqrt{F_{Long}{}^2 + F_{Lat}{}^2}}{F_{Vert}}$$

Traction creep curves were then generated for each friction, vertical load, and roller speed combination by plotting Tc versus AoA. All graphs are presented as "butterfly" plots with both ascending and descending portions of the AoA sweep. The sense of direction in each graph is shown by arrows in Figure 6. Peak saturation Tc values for the negative and positive AoA portions of the sweep were acquired during the up-sweep to the AoA target. These are indicated on each portion of the graph by a red dot.

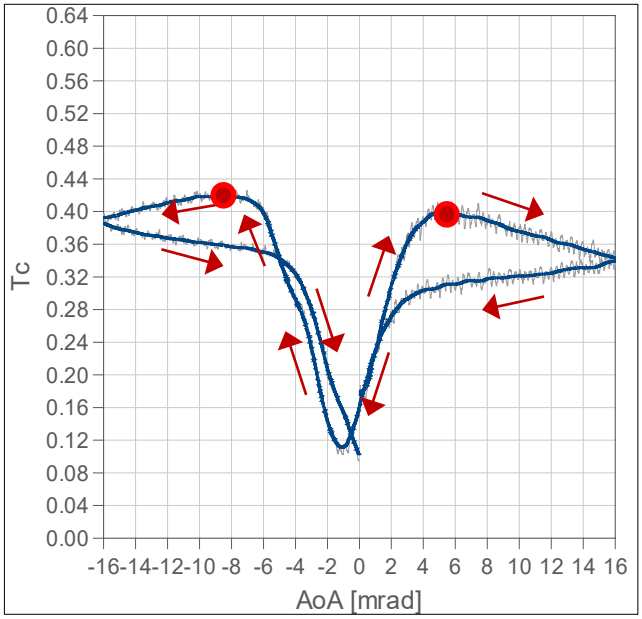

Figure 6. Tc versus AoA plot indicating direction of AoA sweep during testing

3. Results

3.1 Traction Coefficients (Tc)

Individual creep curves for all tested conditions are presented in Figure 7. In each Tc versus AoA plot both ascending and descending portions of the graphs are shown. For all cases, only the ascending portion of the graph was analyzed for the peak creep saturation value, as this was assumed to be the portion of the curve where the W/R interface was saturated to the desired friction level. The peak Tc values are shown in Table 1.

In the descending portion of the curve, the applied friction control material would have partially (or completely) worn off, resulting in higher friction levels. This was true for both the lube and TOR FM stick materials, where the application of high AoA wore off the dry stick material relatively quickly, even though the material was continuously applied during the data acquisition cycle run.

It is evident from the IWS lateral load data that the rate of dry stick material loss was greater than the rate of its deposition on the wheel running surface during testing. As a result, the traction forces rose to levels that were similar to the dry friction runs.

Table 1. Peak (saturation) Tc values for negative and positive AoA sweeps

Negative AoA Sweep

		Tc			
		WET	TOR Stick	LUBE Stick	DRY
Condition	30mph, 37.5kip	0.17	0.40	0.36	
	30mph, 15kip	0.18	0.39	0.41	0.49
	30mph, 10kip	0.17	0.26	0.36	0.49
	10mph, 37.5kip	0.19	0.40	0.39	0.50
	10mph, 15kip	0.20	0.42	0.33	0.55
	10mph, 10kip	0.23	0.28	0.37	0.55
	2mph, 37.5kip	0.24	0.34	0.32	0.44
	2mph, 15kip	0.31	0.33	0.35	0.47
	2mph, 10kip	0.31	0.30	0.44	0.45

Positive AoA Sweep

		Tc			
		WET	TOR Stick	LUBE Stick	DRY
Condition	30mph, 37.5kip	0.11	0.32	0.40	
	30mph, 15kip	0.09	0.31	0.40	0.44
	30mph, 10kip	0.09	0.40	0.38	0.44
	10mph, 37.5kip	0.10	0.30	0.36	0.42
	10mph, 15kip	0.08	0.30	0.34	0.48
	10mph, 10kip	0.09	0.38	0.40	0.42
	2mph, 37.5kip	0.14	0.30	0.34	0.36
	2mph, 15kip	0.22	0.33	0.40	0.36
	2mph, 10kip	0.22	0.21	0.43	0.37

Dry condition, vertical load of **10 kip** at roller speed of **2**, **10**, and **30** mph

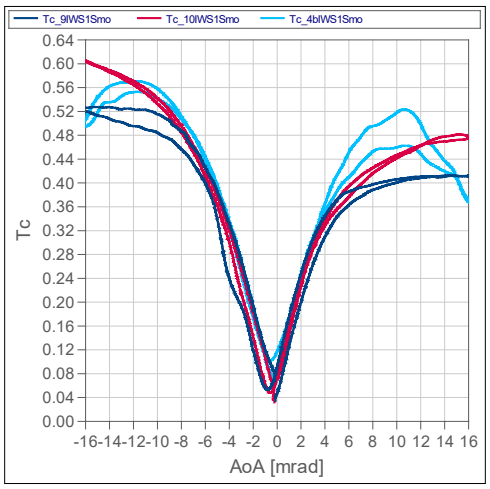

Dry condition, vertical load of **15 kip** at roller speed of **2**, **10**, and **30** mph

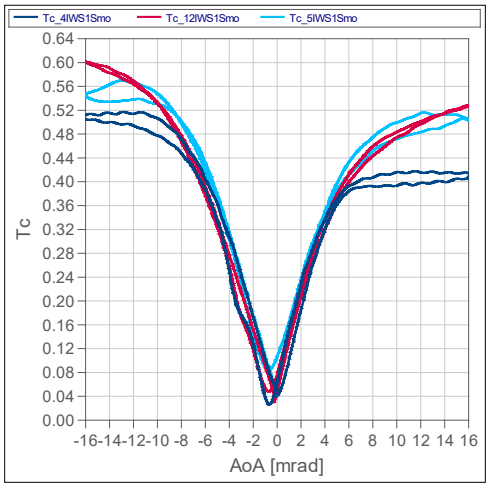

Dry condition, vertical load of **37.5 kip** at roller speed of **2**, and **10** mph

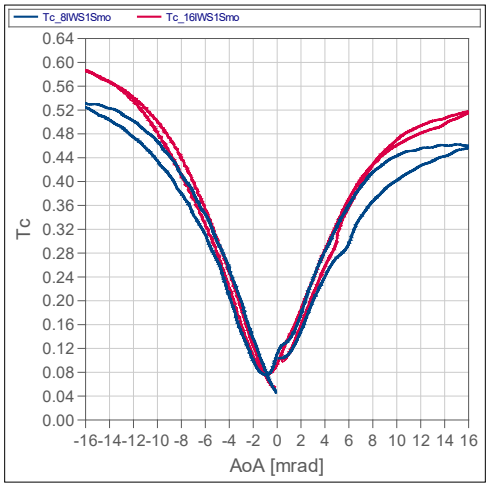

Lube stick condition, vertical load of **10 kip** at roller speed of **2**, **10**, and **30** mph

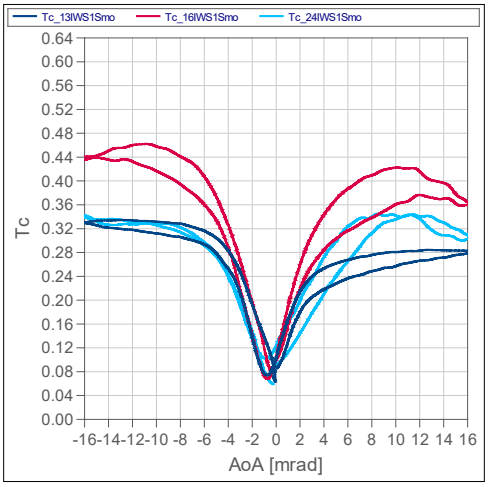

Lube stick condition, vertical load of **15 kip** at roller speed of **2**, **10**, and **30** mph

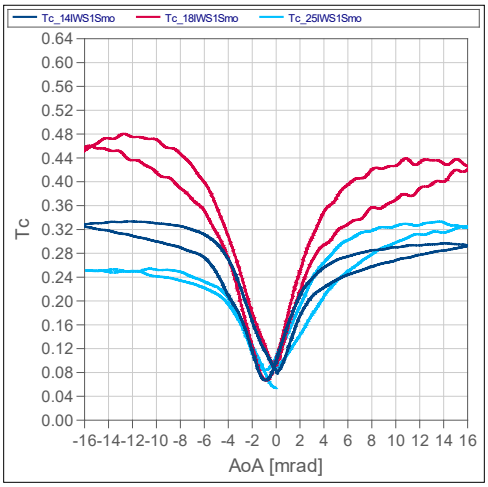

Lube stick condition, vertical load of **37.5 kip** at roller speed of **2**, **10**, and **30** mph

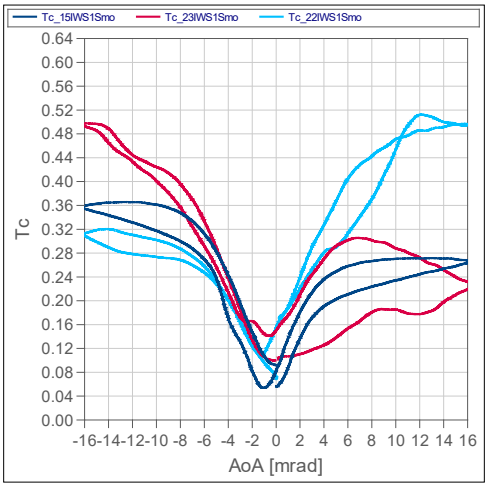

TOR FM stick condition, vertical load of **10 kip** at roller speed of **2**, **10**, and **30** mph

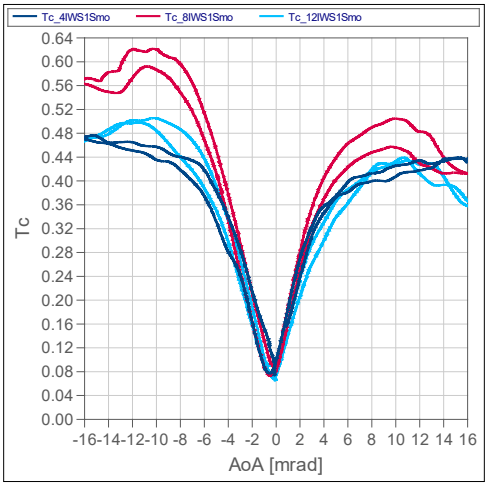

TOR FM stick condition, vertical load of **15 kip** at roller speed of **2**, **10**, and **30** mph

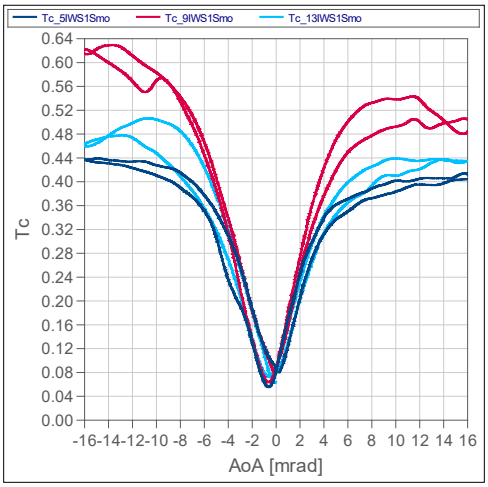

TOR FM stick condition, vertical load of **37.5 kip** at roller speed of **2**, **10**, and **30** mph

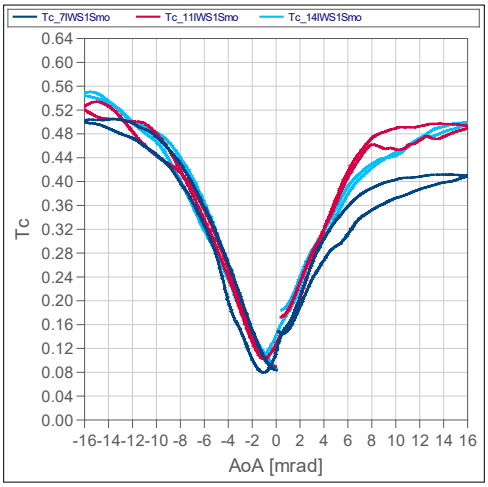

Wet condition, vertical load of **10 kip** at roller speed of **2**, **10**, and **30** mph

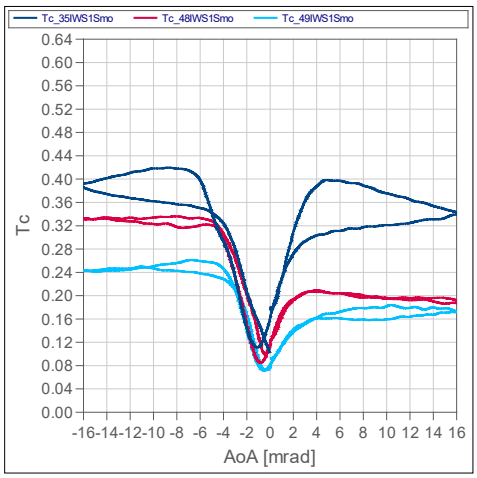

Wet condition, vertical load of **15 kip** at roller speed of **2**, **10**, and **30** mph

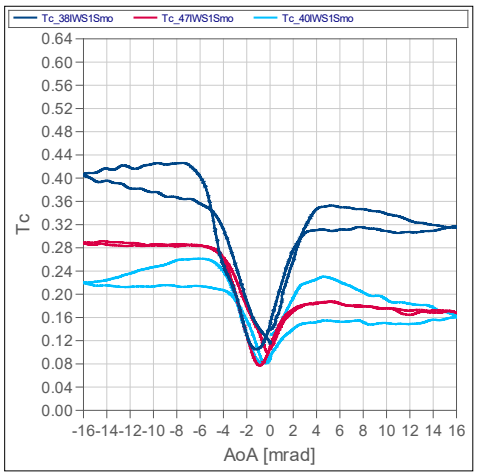

Wet condition, vertical load of **37.5 kip** at roller speed of **2**, **10**, and **30** mph

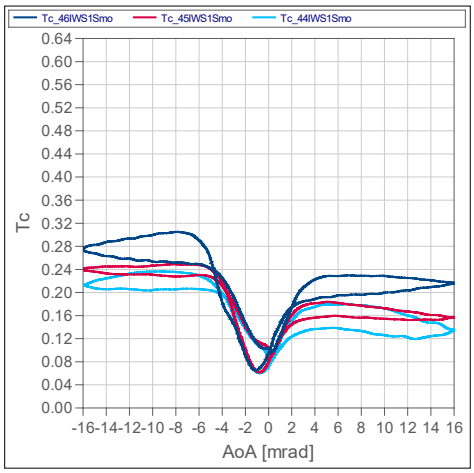

Figure 7. Traction creep curves (Tc versus AoA) as a function of W/R friction conditions, vertical wheel loads and WBB roller speeds applied during testing

When determining the peak saturation level based on the IWS lateral forces for the ascending portion of the curve, the peak value was approximated to be the point where the lateral force level rise stabilized. As seen in Figure 8, this is an approximate value since there was still relatively little noise in the data (post-filtering and smoothing).

The typical trend in the data is indicated in the graph. Wet runs yielded lateral loads that stabilized relatively quickly and then remained stable with the additional application of the AoA. These values were also the lowest of all friction levels investigated. Lube and TOR FM stick application yielded values that were relatively higher than for wet friction, and did not stabilize at any specific AoA. As described earlier, this response is believed to be due to the wearing off of the dry stick material during AoA application, and the inability of the sticks to replenish the material on the wheel surface at a rate equivalent to its removal. Not surprisingly, dry friction yielded the highest IWS lateral load values.

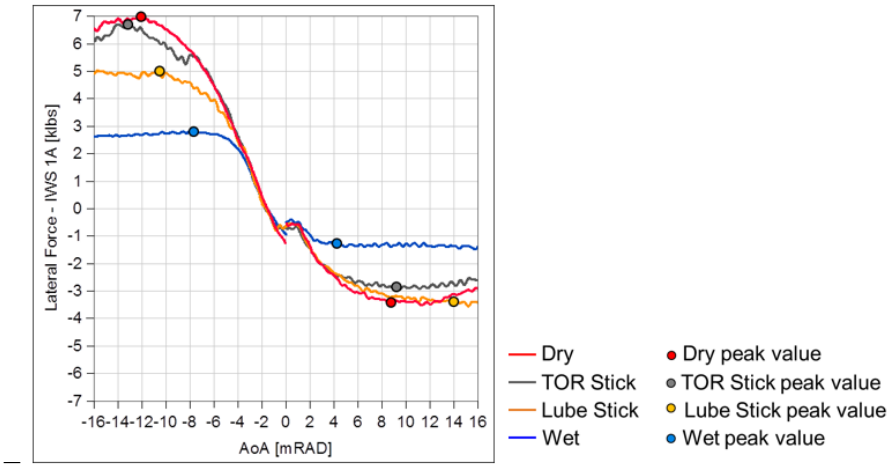

Figure 8. Typical IWS reactive lateral loads versus applied AoA indicating variation in the data as a function of applied friction level and direction of AoA sweep. Only the ascending portion of the AoA sweep is shown in this graph.

Another interesting trend emerged from the data analysis of all runs. The positive AoA travels, as opposed to the negative AoA motion, resulted in lower magnitude lateral loads on the wheelset, as indicated in Figure 8. This was true for all friction conditions investigated, and this behavior is believed to be due to the characteristics of the WBB test rig that have to do with the relative direction of the roller motion combined with the direction of the AoA sweep.

If the AoA application moved the W/R contact patch in the same direction as the roller motion, the IWS lateral forces were higher. However, if the AoA application moved the W/R contact patch in the opposite direction, the IWS lateral forces were lower. The spin creep generated at the W/R interface due to the rotating direction of the roller was affecting the IWS force readout by either adding or subtracting a normal force component (depending on the direction of the AoA sweep relative to rotation of the roller wheel). Additional contribution to these force differences could have come from roller diameter and/or roller profile differences. Since each roller was ground independently there could have been differences in roller diameters and/or roller running surface profiles. Although these differences were believed to be relatively small,

they could have been contributory factors in the observed IWS force differences for negative and positive AoA wheelset sweeps.

In addition, the wheelset's transverse profiles and diameters could have contributed to the variation in IWS lateral force readings. However, since only one wheelset was used in this experiment it was difficult to weigh the importance of wheelset profiles as a contributing factor on the acquired lateral force metrics. Distinguishing between WBB and wheelset setup and the effect each has on the observed differences between lateral force measurements in negative and positive AoA angle sweep, would require more experimentation with a variety of different wheelsets and a comparison of data from all runs to separate clear trends in behavior of the WBB from that of the individual wheelsets. This analysis was not part of the scope of work.

The data in Figure 7 is for the west (W) wheel. The schematic of the relative motion of the wheelset with respect to the roller rotation is shown in Figure 9.

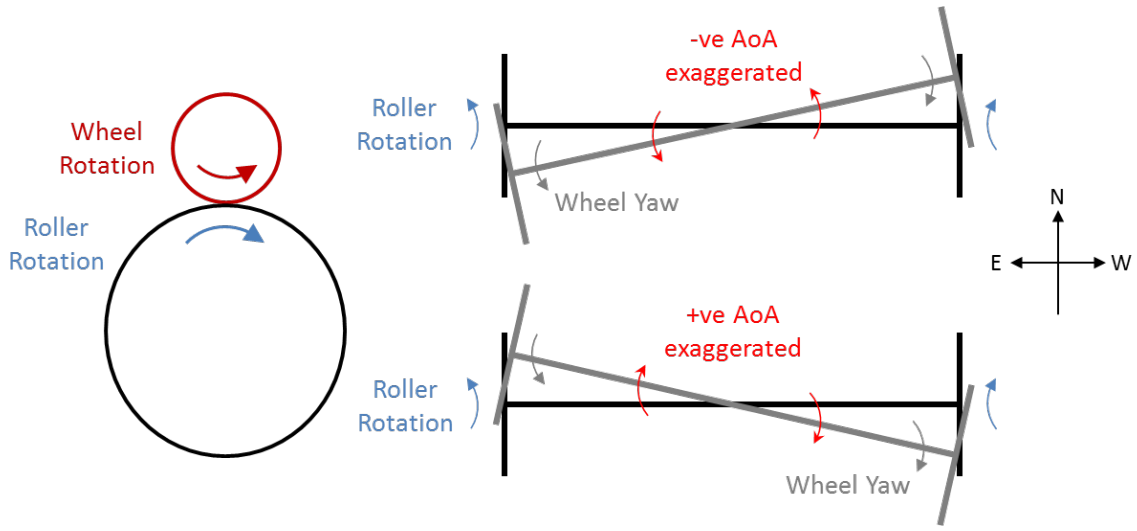

Figure 9. Schematic indicating the WBB wheelset AoA sweep motion in relation to the roller rotation

Figure 10 shows the analysis of peak IWS lateral forces as a function of applied friction conditions, applied vertical loads, and roller speeds. Lateral forces were on average twice as high during the negative AoA sweep than they were during the positive AoA sweep.

Comparison of peak lateral forces as a function of friction condition indicated that dry friction yielded the highest lateral forces at the W/R interface, whereas wet friction yielded the lowest forces, with both lube stick and TOR FM stick application being in between these two extremes. The highest vertical load of 37.5 kip yielded the highest lateral forces, which decreased as the vertical load decreased. This force decrease was less gradual in the wet condition.

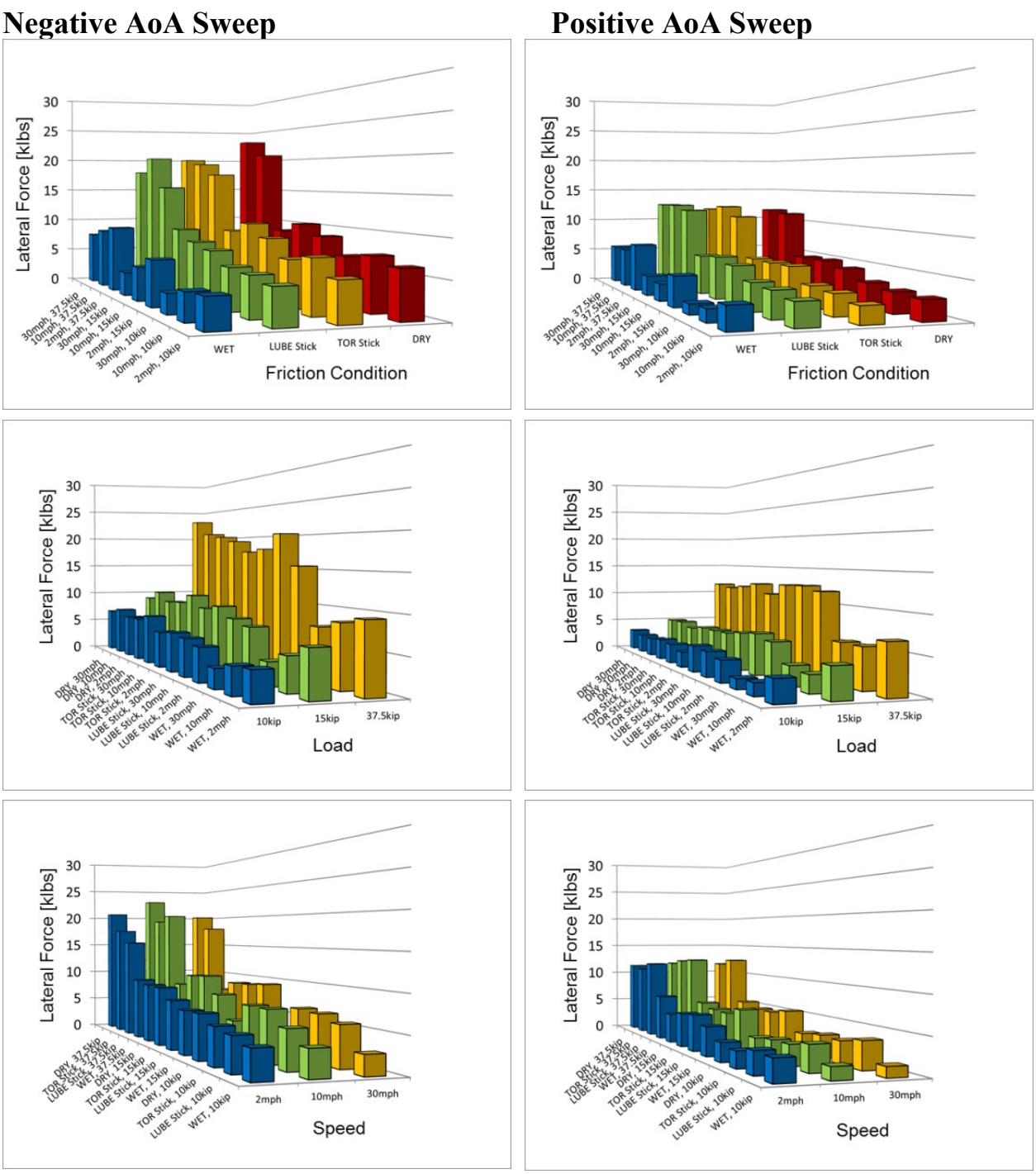

Figure 10. Measured IWS peak lateral force as a function of the friction conditions, load conditions, and roller speeds for negative and positive AoA sweeps

Roller speed, on the other hand, did not appear to have any effect on the lateral forces at any of the friction and load conditions investigated. The response was, on average, flat in the 2–30-mph roller speed range for all frictions and vertical loads applied during testing.

The results also indicated that the application of water at the W/R interface saturated the contact patch early, with lateral force response being flat as AoA increased for both the negative and

positive AoA sweep directions. Application of both lube and TOR FM stick materials, on the other hand, saturated the lateral force at higher AoA values and higher lateral loads. The highest lateral load saturations occurred when the W/R interface was dry.

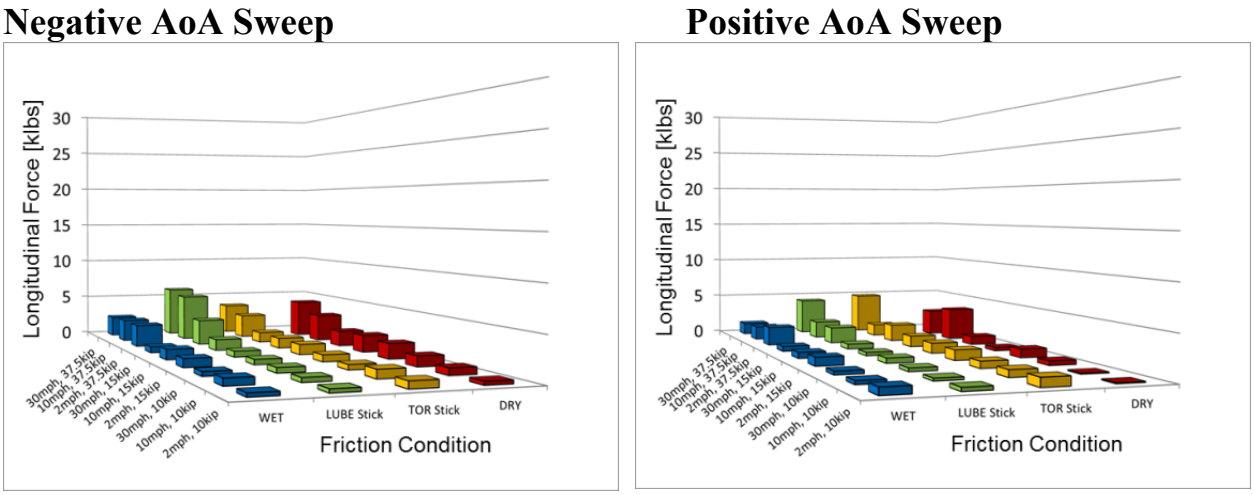

Figure 11. Measured IWS peak longitudinal force as a function of the friction conditions for variable roller speeds and vertical wheelset loads for negative and positive AoA sweeps

Analysis of peak longitudinal forces as a function of friction conditions showed that longitudinal forces were relatively small for all conditions tested (see Figure 11). The measured maximum longitudinal force at 37.5-kip vertical wheel load was approximately 5 kip for the lube and TOR stick conditions. This was most likely due to small differences in the east and west transverse wheel and roller profiles, which caused a small rolling radius difference to develop as the wheelset was yawed. The longitudinal forces were relatively small in comparison to lateral forces on the wheels. However, these values were not ignored in the Tc calculations, as all variables mentioned in the equation were considered in generating creep curves.

As previously explained, all three forces measured by the IWS had contributory effects on the calculation of Tc. The positive AoA sweep yielded, on average, lower Tc values (due to the described WBB characteristics). With this in mind the trends of peak saturation Tc values are presented in Figure 12.

Analysis of these graphs indicated that wet friction condition resulted in the lowest Tc peak saturation values, whereas dry friction yielded the highest Tc peak saturations. Lube stick and TOR FM stick friction conditions had intermediate values.

Tc did not appear to be sensitive to load changes (as was observed with IWS lateral load plots in Figure 10). Peak Tc values remained relatively unchanged in the 10 to 37.5-kip range for the specific friction and roller speed combinations investigated. This was also the case for roller speed variation. Peak Tc was relatively unchanged as a function of roller speed for specific friction and load combinations.

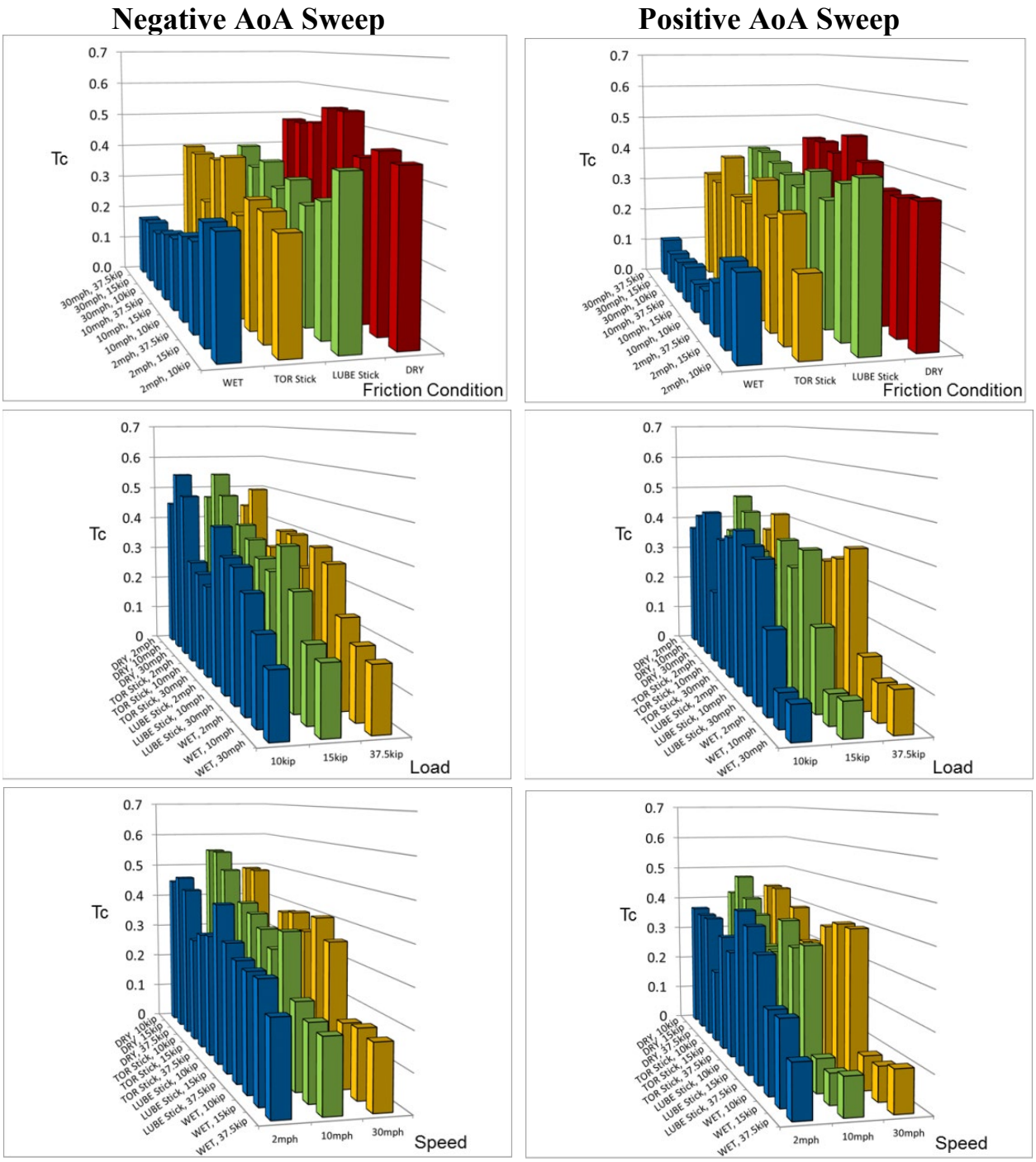

Figure 12. Calculated saturation Tc as a function of the friction conditions, load conditions, and roller speeds for negative and positive AoA sweeps

Readings in the wet friction condition at 2 mph were at times higher than those at 10 and 30 mph roller speeds. This suggested a hydro-dynamic lubrication effect. It is possible that water does not enter the W/R contact patch at lower roller speeds (i.e., 2 mph) in sufficient volume to form a hydro-dynamic film, effectively yielding a contact patch comparable to a “dry” friction condition

(even though the zone surrounding the contact patch might be flooded with water). On the other hand, enough water may be drawn into the contact patch at higher roller speeds to create the hydro-dynamic film, which effectively lowers the Tc values.

Another plausible explanation for this observation is that the use of water at lower roller speeds aids the formation of oxides (i.e., rust) at the W/R interface, which raises the friction level closer to "dry" friction conditions, rather than lubricated target friction. This was substantiated by tribometer measurements presented later on (refer to Section 3.3). In either case, 2 mph roller speeds did not reflect the applied W/R wet friction condition accurately.

3.2 Wear and Rolling Contact Fatigue

During testing the wheelset travelled approximately 410 miles. Initial wheel and roller profiles were compared to the profiles at the end of each friction condition using a MiniProf®. Since the distance travelled was relatively short, the wear on both wheels and rollers was relatively small as well. As a result, only the overlay of initial (pre-test) and final (post-test) profiles on the wheel and roller are presented here (see Figure 13).

The results indicated that there was an approximate 0.2 mm maximum wear in the wheel tread and an approximate 0.1 mm maximum flange wear difference. Maximum wear on top of the roller surface was approximately 0.2 mm (in both cases indicated by an arrow). Both wheel and roller surfaces showed a minimal amount of RCF on the running surface. No other defects were observed anywhere on the surface.

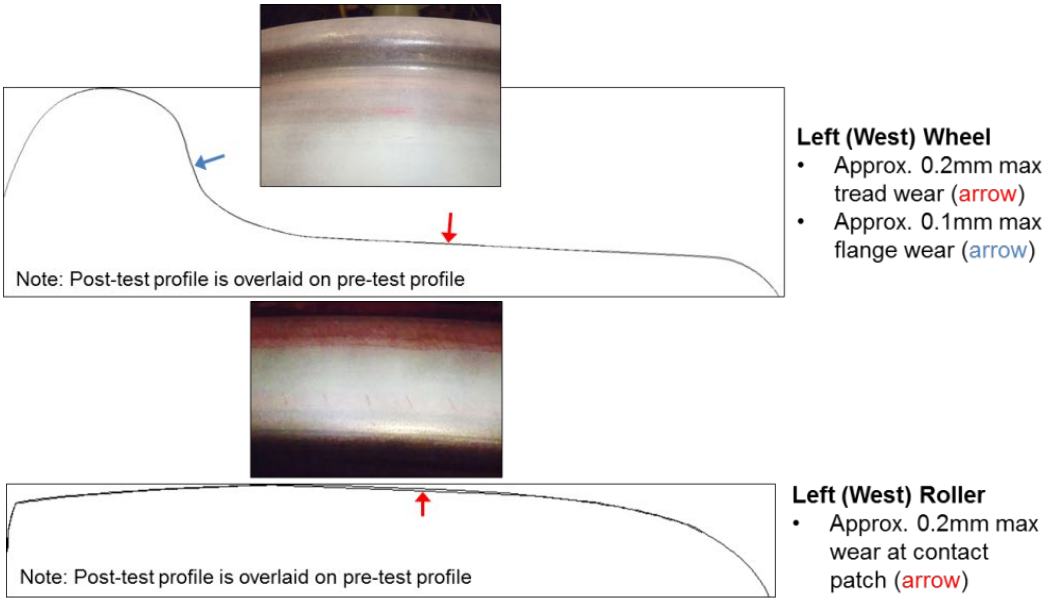

Figure 13. Pre-test and post-test overlay of wheel and roller profiles. Dye penetrant images of wheel and roller conditions following the last (wet) friction test run are as indicated.

This relatively small amount of wear on the wheel tread was due to the short distance travelled as well as the use of dry stick lubrication and friction modification for 50 percent of testing, water for 25 percent of testing, and a dry condition for an additional 25 percent of the testing. The overall amount of testing was not sufficient to cause either excessive wear or RCF on the wheel tread.

Dye penetrant images of the wheel following application of each friction run are shown in Figure 14. These results indicated that there was no RCF present anywhere on the wheel running surface before or after all testing was conducted. The W/R contact patch remained consistent throughout testing of all friction conditions and is clearly identified in each image as a white band running in the middle of the tread surface. This shows that position of W/R contact was constant for all testing conditions.

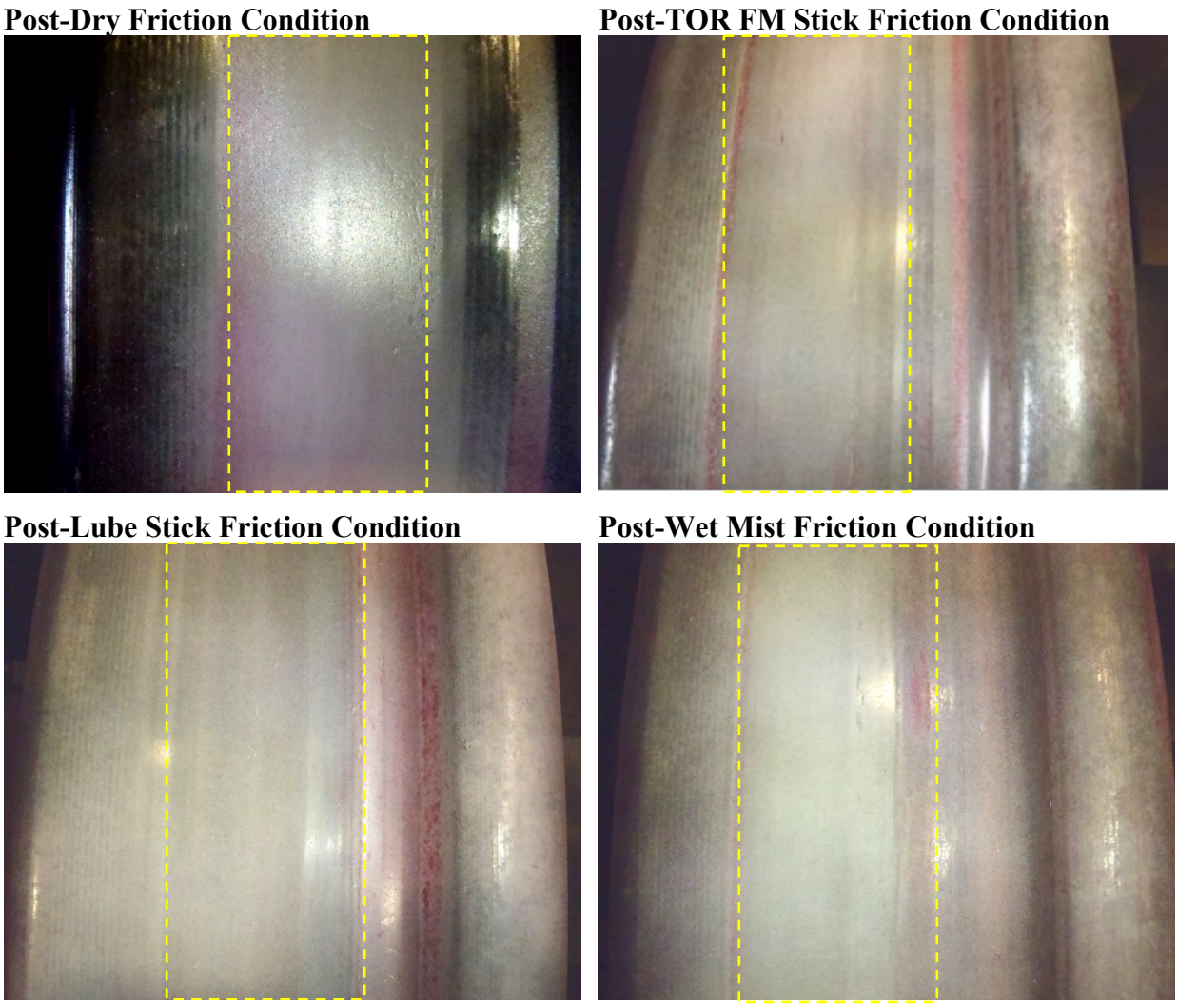

Figure 14. Dye penetrant test results on the wheel surface following testing of each friction condition. W/R contact patch location is indicated in each image by the boxed zone.

3.3 Tribometer

The tribometer setup on the west roller included fixing the position of the bottom of the tribometer frame to ensure uniform swing-arm action between individual runs (see Figure 15).

During product saturation, the wheel rotated in the direction of the red arrow. However, as a result of space limitation at the base of the roller and the setup of the tribometer unit, the wheel turned the opposite way at 2 mph during the tribometer test runs.

This setup was utilized for TOR FM and lube stick applications. The stick material application was simultaneous to both wheels to ensure uniform wheel behavior during AoA sweeps. During wet runs the water mist was applied directly at the W/R contact patch of both wheels. No product was applied during "'dry" runs.

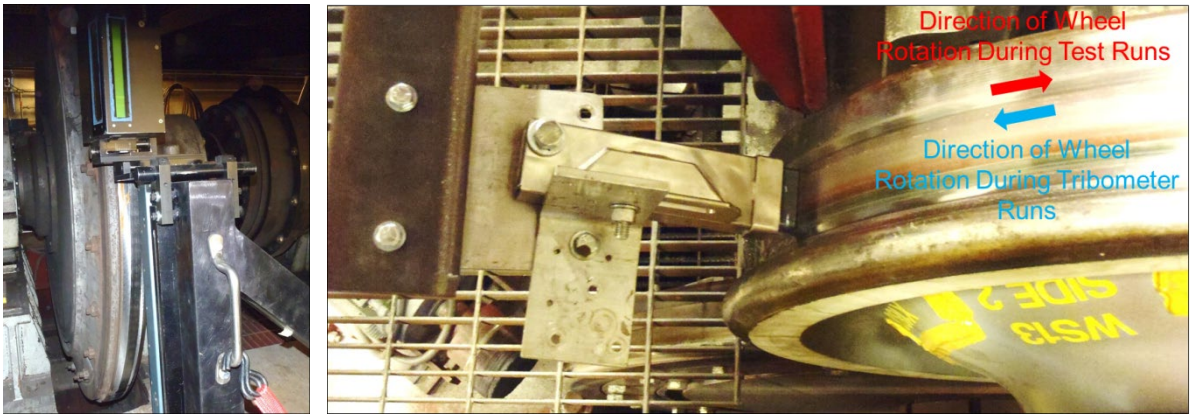

Figure 15. Tribometer setup on the roller, along with lube stick and TOR FM application on wheel tread surface relative to direction of wheel rotation during testing

Figure 16 shows roller friction results as a function of applied AoA and vertical load for the four friction conditions investigated. A ±16 mrad AoA sweep for the dry and wet friction conditions yielded similar values.

As expected, in all cases increasing the wheelset vertical load increased the friction coefficient. In the dry and wet conditions the friction readings were essentially flat in the ±16 mrad AoA sweep range. This was to be expected, as the W/R contact patch remained at an established friction condition during the entire AoA sweep range.

However, for TOR and lube stick applications, the graphs did not display this behavior, and tended to spike upward as either -16 or +16 mrad AoA was approached. This was not entirely true for lower vertical loads, as only portions of the curve for the TOR FM stick application spiked upward, and the lube stick displayed "flat" friction curve behavior. However, this behavior was clearly evident at the 37.5-kip vertical loading condition. These friction readings were most likely due to the availability of the friction stick material at the W/R interface during the entire AoA sweep. When the material's film was established at 0 mrad AoA, the friction value was relatively low, since the stick material was present at the interface.

However, when the AoA sweep was applied the stick material wore off from the interface, and was replenished at the interface at a lesser rate than it was being lost. Essentially, the 2-mph roller speed was inadequate to reapply the friction material at the W/R interface rapidly enough

to compensate for the material loss. When the wheel achieved the extreme AoA of either -16 or +16 mrad, the material loss rate reached the apex, and as a result the friction coefficient measured by the tribometer was the highest. This behavior was most evident at the highest vertical load when the condition resulted in the highest rate of stick material loss from the W/R interface.

On the other hand, this behavior was not evident with either the dry or wet friction conditions, since the W/R interface was always unchanged in the friction target condition. Application of AoA did not deplete the target friction level. The "target friction" in this case was referred to as a value at which friction level stabilized.

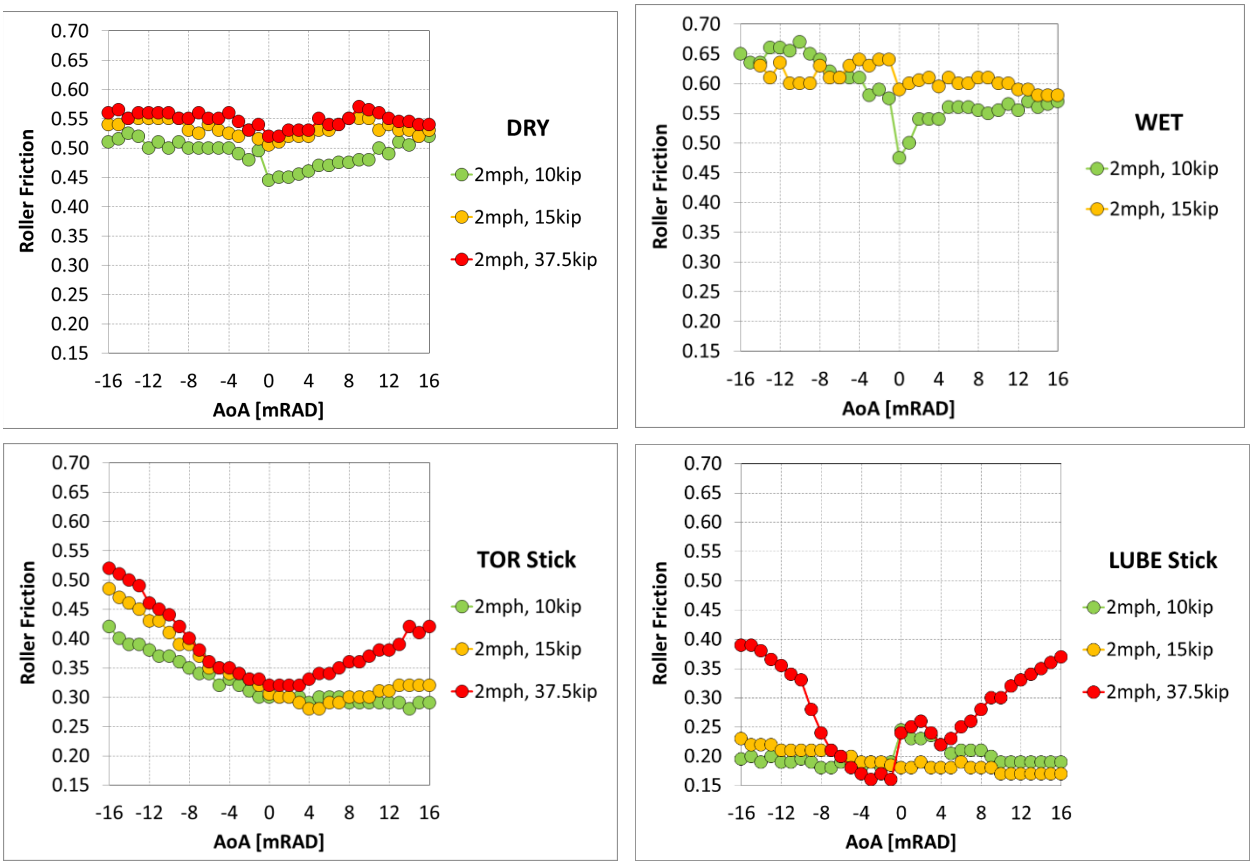

Figure 16. Roller friction results for four investigated friction levels

As explained earlier, measuring wet friction at the 2-mph roller speed is most likely not the best way to measure true wet friction, since at this low speed a water film does not establish itself in the W/R interface. The 2-mph roller speed friction measurements between the push tribometer's rolling wheel and the wheelset wheel substantiated this by yielding friction values on par with, or in some cases higher than, those in the dry friction condition. A more accurate assessment of wet friction would be made at higher roller speeds. However, the push tribometer is only functional at walking speeds (i.e., typical push tribometers were designed for operation at walking speed on track).

All the tribometer coefficient of friction measurements acquired as part of this study were relatively high compared to the condition expected on the roller running surface. In general, push

tribometers tend to read high, often by an additional 0.15, compared to an IWS readout. This is possibly due to calibration and/or noise issues; hardness of mating surfaces that may affect contact behavior; and roughness of the tribometer wheel's running surface (most in-field units have worn surfaces), which will yield more contact area with the measured surface and provide higher readings. The tribometer used in this study was previously utilized on track in the field. As such, the rolling wheel was relatively flat in the contact region due to wear. This might have contributed to the higher friction readings.

4. Conclusion

Work conducted during this test included acquisition of lateral loads through the IWS. These were then used to generate Tc plots as a function of applied AoA. Wheel wear and RCF were assessed for each friction condition, as were tribometer measurements at 2 mph roller speeds.

When considering IWS lateral load results (see Figure 10) the wet runs yielded lateral loads that stabilized relatively quickly and then remained stable with the additional application of the AoA. These values were also the lowest of all friction levels investigated. TOR FM and lube stick application yielded values that were relatively higher than those for wet friction and did not stabilize at any specific AoA. This response was believed to be due to the wearing off of the dry stick material during AoA application and the inability of the stick material to replenish the contact zone on the wheel surface at a rate equivalent to stick material removal. Dry friction yielded the highest IWS lateral load values.

Analysis of the peak IWS lateral forces as a function of the applied friction conditions, vertical loads, and roller speeds indicated that lateral forces were on average twice as high during the negative AoA sweep than they were during the positive AoA sweeps.

The positive AoA travels, as opposed to the negative AoA motion, resulted in lower magnitude lateral loads on the wheelset. This was true for all friction conditions investigated. This behavior was believed to be due to the characteristics of the WBB test rig that involved the relative direction of roller motion combined with the direction of the AoA sweep. When the AoA application moved the W/R contact patch in the same direction as the roller motion, the IWS lateral forces were higher. However, if the motion was in the opposite direction the IWS lateral force were lower. The spin creep generated at the W/R interface due to the rotating direction of the roller was affecting the IWS force readout by either adding (or subtracting) a force component normal to the wheelset rolling plane, depending on the direction of the AoA sweep relative to the rotation of the roller wheel.

Contributions to these lateral force differences could have come from roller diameter and/or roller profile differences. Since each roller was ground independently, there could have been variations in roller diameters and/or roller running surface profiles. Although these differences were believed to be relatively small, they could have been contributory factors in the observed IWS force readouts for negative and positive AoA wheelset sweeps. In addition, the wheelset's transverse profiles could have contributed to the variation in IWS lateral force readings. However, since only one wheelset was used in this experiment it was difficult to weigh the importance of wheelset profile as a contributing factor on the acquired lateral force metrics.

Distinguishing between WBB and wheelset setup, and the effect each had on the observed differences between lateral force measurements in negative and positive AoA angle sweep, would require more experimentation with a variety of different wheelsets. A comparison of data from all runs would be needed to separate clear trends in the behavior of the WBB and that of the individual wheelsets. Unfortunately, this analysis was not part of the scope of this work.

Comparison of the peak lateral forces as a function of friction condition (see Figure 10) indicated that dry friction yielded the highest lateral forces at the W/R interface, whereas wet friction yielded the lowest forces, with both lube stick and TOR FM stick application being in between these two extremes. The highest vertical load of 37.5 kip yielded the highest lateral forces, and

these forces decreased as the vertical load decreased. This decrease was less gradual in the wet condition.

Roller speed on the other hand did not appear to have any effect on the lateral forces at any of the friction and load conditions investigated. The response was on average flat in the 2–30 mph roller speed range for all frictions and vertical loads applied during testing.

The results also indicated that application of water at the W/R interface saturated the contact patch early, with lateral force response being flat as AoA increased for both the negative and positive AoA sweep directions. Application of both lube and TOR FM stick material, on the other hand, saturated the lateral force at higher AoA values and higher lateral loads. The highest lateral load saturations occurred when the W/R interface was dry.

Measured longitudinal forces were relatively small for all conditions tested (see Figure 11). However, these values were not ignored in the Tc calculations, as all variables mentioned in the Tc equation were considered in generating the creep curves. All three forces measured by the IWS contributed to the Tc calculations.

Analysis of Tc graphs indicated that the wet friction condition resulted in the lowest Tc peak saturation values where dry friction yielded the highest Tc peak saturation (see Figure 12). Lube stick and TOR FM stick friction conditions had intermediate values.

Peak saturation Tc did not appear to have been sensitive to load changes (as was observed with IWS lateral load plots). Peak Tc values remained relatively unchanged in the 10 to 37.5-kip range for the specific friction and roller speed combinations investigated. This was also the case for roller speed variation. Peak Tc was relatively unchanged as a function of roller speed for specific friction and load combinations.

Peak Tc readings in the wet friction condition at 2 mph were at times higher than those at 10 and 30 mph roller speeds. This suggested a hydro-dynamic lubrication effect. It is possible that water did not enter the W/R contact patch at lower roller speeds (i.e., at 2 mph) in sufficient volume to form a hydro-dynamic film, effectively yielding a contact patch comparable to a “dry” friction condition (even though the zone surrounding the contact patch might have been flooded with water). On the other hand, enough water may have been drawn into the contact patch at higher roller speeds to create the hydro-dynamic film, which effectively lowered the Tc values. Using water at lower roller speeds might have also aided the formation of oxides (i.e., rust) at the W/R interface which raised the friction level closer to “dry” friction conditions, rather than lubricated target friction. These observations were substantiated by the tribometer measurements (see Figure 16). In either case, 2 mph roller speed was not adequate in reflecting the applied W/R wet friction condition accurately.

Measurements of wheel and roller wear indicated that maximum wear in both the wheel tread and top of roller surface was approximately 0.2 mm (see Figure 13). Observation of wheel and roller running surfaces post-test indicated minimal amount of RCF on the running surfaces of both wheel and roller, with no additional defects observed anywhere on either contact surface (see Figure 14). This small amount of wear and absence of RCF can be explained by the relatively short distance travelled by the wheelset during testing (at a total of 410 miles).

Tribometer measurements at all friction conditions showed that increasing the wheelset vertical load increased the friction coefficient (see Figure 16). In dry and wet conditions, the friction readings were essentially flat, in the ±16 mrad AoA sweep range. This was to be expected, as the

W/R contact patch remained at established friction conditions during the entire AoA sweep range.

For TOR FM and lube stick applications the graphs did not display this behavior, and for the most part they spiked upward as either -16 or +16 mrad AoA was approached. This was not entirely true for lower vertical loads, as only portions of the curve for the TOR FM stick application spiked upward, and the lube stick displayed "flat" friction curve behavior. However, this behavior was clearly evident at the 37.5-kip vertical loading condition. These friction readings were most likely due to the availability of the friction stick material at the W/R interface during the entire AoA sweep. When the material's film was established at 0 mrad AoA, the friction value was relatively low, since the stick material was present at the interface.

When the AoA sweep was applied the stick material wore off from the interface and was replenished on the interface at a lesser rate than it was being lost. Essentially the 2-mph roller speed was inadequate to reapply the friction material at the W/R interface rapidly enough to compensate for the material loss. When the wheel achieved the extreme AoA of either -16 or +16 mrad the material loss rate reached the apex, and as a result the friction coefficient measured by the tribometer was the highest. This behavior was most pronounced at the highest applied vertical loading as a result of highest rate of loss of the deposited stick material from the wheel tread surface.

On the other hand, this behavior was not evident with either the dry of wet friction conditions, since the W/R interface was always unchanged in the friction target condition. Application of AoA did not deplete the targeted friction level. The "targeted friction" in this case is referred to as a value at which the friction level stabilizes.

As explained above, measuring wet friction at the 2-mph roller speed was most likely not the best way to measure true friction, since at this low speed the water film did not establish itself in the W/R contact patch. As a result, a more accurate assessment of wet friction would have been made at higher roller speeds. However, the push tribometer utilized for friction measurements during this study is only functional at walking speeds (i.e., approximately 2 mph). Therefore, higher roller speeds were not an option for friction assessment in this case.

All the tribometer coefficient of friction measurements acquired as part of this study were relatively high compared to the condition expected on the roller running surface. In general, push tribometers tend to read high, often by an additional 0.15 compared to an IWS readout. This is possibly due to calibration and/or noise issue; hardness of mating surfaces that may affect contact behavior; and roughness of the tribometer wheel's running surface (most in-field units have worn surfaces), which will yield more contact area with the measured surface and provide higher readings. The tribometer used in this study was previously utilized on track in the field. As such, the rolling wheel was relatively flat in the contact region due to wear. This may have contributed to the higher friction readings obtained during the testing.

References

1. Eadie, T. D., et al. (2008). The effects of top of rail friction modifier on wear and rolling contact fatigue: Full-scale rail-wheel test rig evaluation, analysis and modelling. *Wear, 265*(9-10), 1222–1230.
2. Igwemezie, J. (2014, January 4). Understanding the Effects of Track Gauge, Wheel/Rail Geometry and Friction on Stresses at the Wheel/Rail Interface. *Interface: The Journal of Wheel Rail Interaction*.
3. Chowdhury, M. A., et al. (2013). *Experimental investigation of friction coefficient and wear rate of stainless steel 202 sliding against smooth and rough stainless steel 304 counter-faces*. *Frictional Wear Resistance, 1*(3).
4. Fletcher, D. I., & Lewis, S. (2013). Creep Curve Measurements to Support Wear and Adhesion Modelling, Using a Continuously Variable Creep Twin Disc Machine. *Wear, 298,* 57–65.
5. Beagley, T. M., McEwen, I. J., & Pritchard, C. (1975). Wheel/Rail Adhesion–The Influence of Railhead Debris. *Wear, 33,* 141–152.
6. Beagley, T. M., & Pritchard, C. (1975). Wheel/Rail Adhesion–The Overriding Influence of Water. *Wear, 35,* 299–313.
7. Hardwick, C., Lewis, R., & Olofsson, U. (2013, July 29). Low Adhesion Due to Oxide Formation In the Presence of Salt. *Proceedings of the Institution of Mechanical Engineers, Part F: Journal of Rail and Rapid Transit*.
8. Lundberg, J., et al. (2015). Measurements of friction coefficients between rails lubricated with a friction modifier and the wheels of an IORE locomotive during real working conditions. *Wear, 324–325,* 109–117.

Abbreviations and Acronyms

AoA	Angle of Attack
AST	Automotive and Surface Transportation
CoF	Coefficient of Friction
FRA	Federal Railroad Administration
FM	Friction Modification
GF	Gage Face
Hz	Hertz
IWS	Instrumented Wheelset
kip	Kilopound
mrad	Milliradian
NRC	National Research Council Canada
PSD	Power Spectral Density
RCF	Rolling Contact Fatigue
TOR	Top-of-Rail
Tc	Traction Coefficient
WBB	Wheel Bearing Brake
W/R	Wheel/Rail